International Journal of Technology and Engineering Studies
volume 7 issue 1 pp. 17-26 doi: https://dx.doi.org/10.20469/ijtes.7.10003-1

Design and Optimization of Portable Small Scale Horizontal Axis Wind Turbine

Monis Sherwa
National University of Sciences & Technology, Islamabad, Pakistan

M. Nasir Bashir
National University of Sciences and Technology (NUST), Islamabad, Pakistan

Muhammad Jameel Wattoo
National University of Sciences & Technology, Islamabad, Pakistan

Muhammad Osama Saeed
National University of Sciences & Technology, Islamabad, Pakistan

Tayyab Naeem
National University of Sciences & Technology, Islamabad, Pakistan

Muhammad Nauman Nawaz
National University of Sciences & Technology, Islamabad, Pakistan

Muhammad Shakeel
National University of Sciences & Technology, Islamabad, Pakistan

Abstract: Large-scale Wind Turbines (LSWTs) are under study for a considerable length of time yet just a couple studies are done on the Small Scale Wind Turbines (SSWTs) particularly for the applications near ground level where wind speed is moderate all together of few meters for each second. The goal of this venture is to outline a little wind turbine that is upgraded for the necessities that accompanied private utilization. The outline procedure incorporates the choice of the wind turbine type and the determination of the blade aerofoil, pitch angle distribution along the radius, and chord length distribution along the radius. The pitch angle and chord length distributions are optimized based on conservation of angular momentum and theory of aerodynamic forces on an aerofoil. Blade Element Momentum (BEM) theory is first inferred and afterward used to direct a parametric review that will decide whether the improved estimations of blade pitch and chord length makes the most productive blade geometry. At last, at least two unique aerofoils will be dissected to figure out that which aerofoil makes the most effective wind-turbine-blade. Afterwards, CFD investigation of the wind turbine is led in Ansys Fluent. The project incorporates a dialog of vital limitations in wind-turbine cutting edge configuration for boosting proficiency.

Keywords: *Horizontal axis wind turbine, drag of wind turbine, lift of wind turbine*

Received: 10 October 2020; ***Accepted:*** 7 December 2020; ***Published:*** 27 February 2021

I. INTRODUCTION

Wind power generation is defined as a process in which wind is harnessed to generate mechanical power which is then utilized to generate electricity. This process is done by utilising the kinetic energy of wind. Kinetic-energy of wind is converted into mechanical energy by using wind turbines. Generally, a wind turbine will have blades that are attached to an input shaft & once wind blows past the blades, it will cause rotation of the turbine which is connected to a generator. A generator produces power through utilization of a magnet & copper coil. Small-scale wind turbines (SSWTs) can work at low wind speed, produce negligible noise & there are no known safety hazards. Regardless of a few points of interest, not very many small-scale wind turbine models have been created.

II. MATERIALS AND METHODS

A wind turbine basically had three main components:

- Rotor which contains blades along with hub.

- System for transmission that contains connecting shafts along with bearings & gears.
- The major component generator.

As the output power of SSWTs is relatively low, even a minute reduction in efficiency because of any of above components can greatly affect the collective performance & usefulness of the wind turbine. All the above components must be designed along with optimization & mutual synchronization in such a way that they will operate at their specified operating condition. There are only few attempts seen in literature related to study of performance characteristics of SSWTs. [1, 2, 3, 4, 5, 6] compared the rates of rotation & coefficients of power of different 31 cm circular diameter wind turbine rotor models. These models were manufactured by making use of four different NACA aerofoils (NACA-0012, NACA-4412, NACA-4415, & NACA-23012). Different geometric constraints like blade angle, blade pitch & number of blades of those turbine models had been examined at various wind speeds. It was detected that rotor having NACA-4412 profiles with 0 angle of twist with 5 angle of blade, & with only two blades gaving the highest rate of rotation although the model having NACA-4415 profile with 0 angle of twist, 18 angle of blade, & having 4-blades gave the maximum coefficient of power. Mathematical work by means of Blade-Element-Momentum (BEM) theory & wake theory was conducted by [7, 8, 9, 10, 11] to evaluate the effects of number of blades & solidness on performance of 1 m radius wind & turbine.

This study recommended that by enhancing the solidness from the predictable range of 5%7% to 15%25% we can attain higher coefficient of power values. Leung et al. optimized various parameters of blades of 23.4 cm diameter turbine using the computational fluid dynamics. The model used in that study had a fan-type, constant-thick (constant thickness along the radius) & numerous blade number rather than conventional aerofoil type having tapered blades. This study braced the element that higher solidity provides improved performance to a SSWT, yet it was as well recommended that blades must not fully reside in the swept area of turbine rotor to avoid obstruction. It can also be detected that all these studies mainly focused on designing & optimizing the rotor of wind turbine, more precisely the blades of turbine. They lack in inclusive generality addressing all parts composed to develop a complete small-scale wind turbine. Probably, the first attempt to make a complete SSWT was performed by [12, 13, 14, 15, 16]. He established a 4-bladed 25cm radius small-wind-turbine called F500 by means of NACA-2404 aerofoil. That turbine showed very decent performance with coefficient of power of 0.36 & having an overall efficiency of 0.25 at the wind speed ranging between 8m/s to 12 m/s.

III. METHODOLOGY

A. *Efficiency of Wind Turbine*

Wind turbine effectiveness is measured by a non-dimensional value called the coefficient of power Cp, which is ratio of power extracted from wind P, to the total power in wind covering the turbine area. Below Equation [17] indicates that Cp is a function of the air density , the area covered by the turbine blade A, and the wind speed v1.

$$\mathrm{Cp} = \mathrm{P} / \left(0.5 * \rho * \mathrm{A} * \mathrm{V}\text{^}3\right) \quad (1)$$

Betz's law demonstrates the extreme power that can be generated from the wind, autonomous of the design of a wind turbine in open stream. As stated by Betz's law, no turbine can catch more than 16/27 (59.3%) of the kinetic energy in wind. The component 16/27 (0.593) known as Betz's coefficient.

B. *Turbine Style*

The two prevailing types of wind turbine are drag and lift type devices. The wind turbine decided for this project is lift-type HAWT because lift-type wind turbine have the possibility to generate more power than drag-type units and for the HAWT a beginning motor is not required. An additional profit of picking a horizontal axis, lift-type wind turbine is that they are the widely used turbine which supports its design data.

C. *Blade Selection*

In this project we have studied various NACA aero foils like 4412, 0012 and 23012 and then selected NACA 23012 based on Gliding ratio as shown in the below graph.

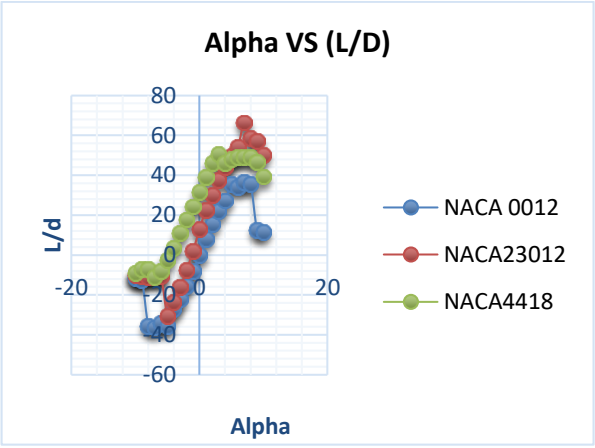

Fig. 1. Gliding ratio comparison of between NACA 0012, NACA2012 and NACA4418

D. Design of Blade Procedure

For efficient designing of wind turbine, we need to consider the material strength and contours of blade must take benefit of aerodynamic considerations. Wind turbine blade contour parameters as well as load test for its integrity of structure can be optimized by considering the aerodynamics properties of turbine blade. We investigated aerodynamics parameters in our study.

How extraction of power from the wind is possible we need some definitions; the conservation of linear momentum and Bernoullis principle were used to arrive at the Betz limit. Comprehensive model developed by Schmitz for the flow in the rotor plane which was based on law of conservation of angular momentum [18]. This method for power calculation will be reviewed in the following section and it will be used to determine the most efficient chord length and pitch angle. We analysed the blade element Momentum theory with the help of pitch angle and chord length distribution which is use for a wind turbine performance evaluation under different conditions.

E. Chord Length and Blade Twist

Air creates the torque on the turbine and with turbine Angular velocity we can calculate power. Torque only produces in wind turbine if there is downstream wake rotation opposite to direction of rotor rotational plane, stated by conservational law. Relative Tangential speed of Rotating blade can be given by following expression as we know that direction of wake produce by torque will be in opposite direction. Tangential wind speed will experience by Blade due to the average clockwise wake velocity can be cater by following term.

F. Batching of Materials

The surface saturated dry aggregates were useful for the concrete mixes under investigation. Cement and aggregates were collected by weight while water was collected in batches by volume. Most of the replacements for the coarse aggregate have been made on a volume basis. To develop the necessary volume of concrete to be produced, the total amount of test samples must be primarily determined. Hence, the samples required were as follows: 18 cylinder samples for compressive strength test = 0.107m

$$\mu = r\omega + \frac{1}{2}\Delta u \tag{2}$$

The tangential interference factors a tell us the increase in tangential speed on the turbine blade due to wake and expressed as.

$$u = r\omega\left(1 + a'\right) \tag{3}$$

Wind turbine relative velocity W components in the upstream and in the downstream. These two components are in the plane of wind turbine. In the upstream there is no wake so rotational velocity is zero, but in the downstream, there is wake and have a rotational velocity of w acting in the opposite direction of the turbine. w/2 is the rotational average velocity due to wake rotation over blade.

Axial interference and tangential interference factor dependence upon the angle formed between plane of rotor and relative wind velocity. Before the rotational plane, variables with subscript 1 represent values and the variables without a subscript shows the values after the rotational plane. If we compare of two diagrams a and b), we get to know that if we decrease the relative wind angle it will cause increase in tangential velocity. Geometric relation is applied in Fig. 4 which are as shown in below. An increase in relative wind speed in terms of in initial relative speed and change in relative wind angle is given by following relation.

$$\Delta w = 2w_1 \sin\left(\varphi_1 - \varphi\right) \tag{4}$$

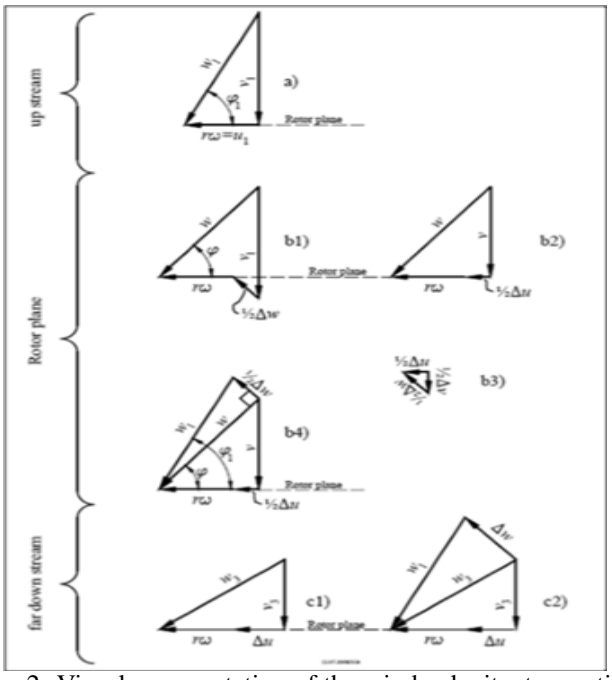

Fig. 2. Visual representation of the wind velocity, tangential velocity, and relative velocity a) upstream, b) in the plane of the rotor, and c) down stream [4]

Applying the law of conservation of momentum, the following equation defines the relation of the lift force for section of blade to the change in relative wind velocity w and mass flow rate of air through a ring having a width dr at radius r from the hub.

$$dF_L = \Delta w dq \tag{5}$$

To calculate the power obtained from the lift force for a segment, the torque is calculated by considering the tangential component of the lift force and by multiplying it with the small blade segment radius. It has been assumed that the drag force of the air foil is almost zero which, if considered, would produce a torque in the opposite direction and reduce the overall power generated.

$$dT = dF_L \sin(\varphi) r \Delta w dq \sin(\varphi) \tag{6}$$

By substituting the expression for mass flow rate of air through the ring element

$$dq = 2\rho\pi r dr v \tag{7}$$

and by submitting the equation for change in rotational velocity w using above relation, the following equation is for the power of a blade segment is calculated.

$$dP = r^2 \omega \rho 2\pi dr w_1^2 \sin\left[2(\varphi_1 - \varphi)\right] \sin^2(\varphi_1) \tag{8}$$

To calculate the angle of relative wind to the rotor plane which produces the maximum power, the derivative of above Equations is taken with respect to and solved equated to zero. When d (dP)/d = 0,

$$\varphi = \frac{2}{3}(\varphi_1) \tag{9}$$

Using the geometric relationship of the tip speed ratio X, most of power can be obtained at the following angle between the relative wind and the plane of rotation.

$$\varphi = \frac{2}{3}\arctan\left(\frac{1}{\omega r}\right) = \frac{2}{3}\arctan\left(\frac{\pi}{Xr}\right) \tag{10}$$

To convert the most efficient wind angle to the pitch angle of the blade , value of must be subtracted from the attack angle . The equation of the optimal pitch angle defined by Schmitz theory is.

$$\beta(r) = \frac{2}{3}\arctan\left(\frac{R}{Xr}\right) - \alpha_D \tag{11}$$

The best distribution of chord length as function of radius can be determined by below equation.

$$dF_L = \Delta w dq = \left[2w_1 \sin(\varphi_1 - \varphi)\right](2\rho\pi r dr)v \tag{12}$$

Using an equation derived from diagram b4) in diagram 2 for axial velocity in the rotor plane v and putting Equation 12 from aerodynamic foil theory, [19] concludes at the following expression for optimal chord length c as a function of blade radius r.

$$c(r) = \frac{1}{B}\frac{16\pi r}{C_L}\sin^2\left(\frac{1}{3}\arctan\left(\frac{R}{Xr}\right)\right) \tag{13}$$

Using this equation, the blade is made in a way to provide maximum output. The blade pitch is distributed along its radius to ensure the fact that the relative wind direction is intercepting the blade at the required angle of attack. The length of chord is optimized to provide maximum lift along the blade radius. While the output is dependent on the assumptions. More accurate the assumptions, more accurate the output will be. For parameters such tip speed ratio, there is not signal optimal value, multiple values can be used to find a trend.

Fig. 3 and 4 below are used to compare the optimized pitch angle and chord length distribution obtained by Betz and Schmitz, respectfully. The value of difference in pitch angle is highest at the hub of the blade, with a difference of about 20 degrees at 5% of the blade length. The difference decreases until after about 50% of the blade length when the two lines are within a degree of one another. Since the hub of the turbine will likely consume the first 10% of the blade, it appears that there is a small variation in the results, regardless of the method.

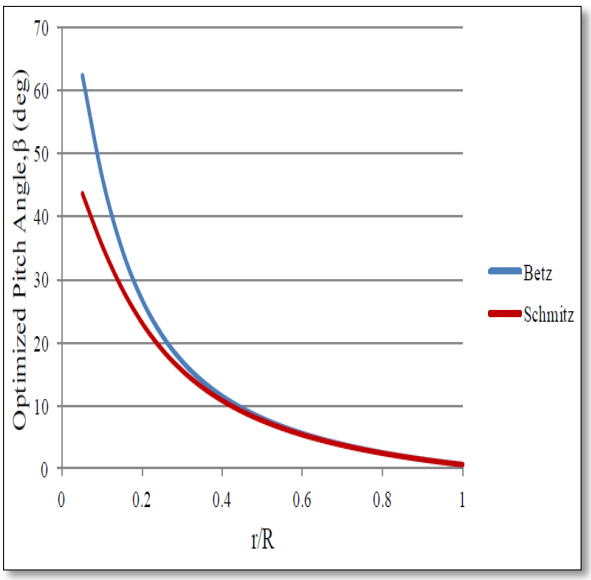

Fig. 3. Comparison of pitch angles calculated with Betz and Schmitz methods

Fig. 4 below shows that chord length variation between the Schmitz and Betz methods are larger than pitch angle distributions. Like pitch angle distributions, the difference is more near the base of blade and decreases moving outward. As stated by Betz method, the blade become progressively thick as it goes toward the hub, where the Schmitz method begin slim closest to the hub, achieves a maximum value at about 15% of length of the blade and starts to diminish once more. Unlike for pitch

angles, the chord length distributions seem great outside of the hub area to have an appreciable impact on turbine effectiveness.

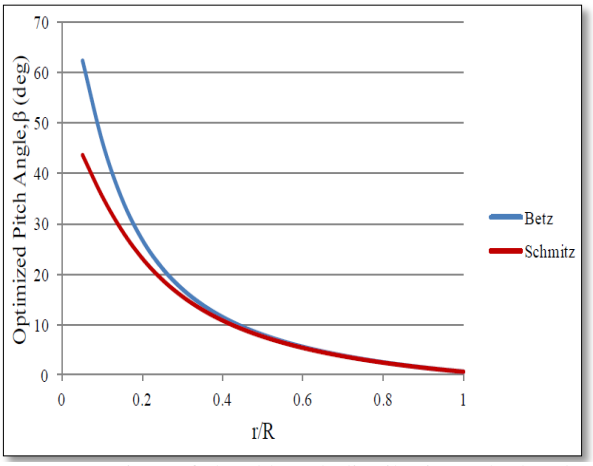

Fig. 4. Comparison of chord length distribution calculated with Betz and Schmitz methods

G. *Blade Element Momentum (BEM) Theory*

Momentum theory and blade element theory are the two main parts of BEM. Flow velocity and ideal efficiency can be found using momentum theory which may be used for finding the forces acting on the rotor to produce fluid motion. Momentum theory does not depend upon blade geometry so it will not be able to select blade parameter. We can find the forces on the blade due to fluid motions in terms of geometry of blade using blade element theory. These two theories combine to form Blade element theory that rotor geometry to the rotor performance.

We made the following assumptions for the blade element theory and momentum theory. our assumptions for momentum theory are written below.

- Frictional drag will not be considered during blade operation.
- Well defined slipstream separates the flow passing through the outer disc from that rotor disc.
- For the undisturbed free stream static pressure remains same so we can assume that inlet pressure at far ahead of inlet and outlet at far behind will remain same.
- Rotor disc have uniform thrust loading.
- The disc will not impart any rotation to the flow.

In blade element theory we made the following assumptions:

- Along the blade there will be no interference between successive elements of blade.
- Only considered those forces which are acting on the blade element due to drag and lift characteristics of blade element sectional profile.

Next, we set the expression for differential thrust using blade element theory to the given equation for differential thrust from momentum theory.

$$dT_h = 2\pi r\rho v_2 (v_1 - v_3)\, dr \tag{14}$$

we get the following two relations necessary for BEM theory.

$$\frac{a}{a-1} = \frac{\sigma C_y}{4\sin^2(\varphi)} \tag{15}$$

In next step we equate the equation of differential torque from angular momentum theory to the differential torque using element theory.

$$dT = 2\pi r^2 \rho v_2 u_2 dr \tag{16}$$

get another equation for BEM theory.

$$\frac{a'}{a'+1} = \frac{\sigma C_x}{4\sin(\varphi)\cos(\varphi)} \tag{17}$$

The following expression defined the solidarity ratio.

$$\sigma = \frac{cB}{2\pi r} \tag{18}$$

At the beginning we do not have much information about tangential and axial interference factor as they are function of relative wind angle to the rotational plane which also depend upon interference factors. Axial interference factor shows how much decrease (fractional) in linear wind velocity between rotor plane and free stream while tangential interference factors a increase in tangential wind speed because of blade counter rotating wake. By assuming the values for axial and tangential interference factors as they are initially required for BEM process calculations, however with each iteration the factors will converge, and we get the final values.

BEM theory usually does not consider the phenomena of shed vortices with the blade flow near tip of the blade. The pressure at below side of the blade will continue to decrease relative to pressure on the upper side. At blade tip, the flow of air radial inward over the tip which causes reduction in air circulation which effect cause

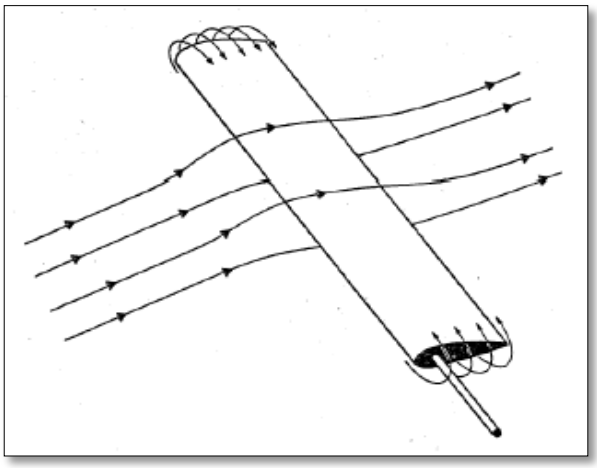

Fig. 5. Comparison of chord length distribution calculated with Betz and Schmitz methods

Tip losses have a major effect to the overall wind turbine performance, and we know that chord length of blade is least at it tip due to distance from hub. Loss of torque due to tip loses can be accounted by a methodology (radial flow effect can be approximate near the blade tip) developed by the Prandtl and this methodology is quite good for high tip speed ratios and for turbines having more than two blades. The factor derived by Prandtl is defined:

$$F_P = \frac{2}{\pi}\cos^{-1}\left(e^{-f}\right) \tag{19}$$

$$f = \frac{B}{2}\frac{R-r}{r\sin(\varphi)} \tag{20}$$

considering the Prandtl tip loss correction during solving of Equations we get the two final equations which further used in procedure of BEM.

$$a = \frac{1}{\left(\frac{4F_P\sin^2(\varphi)}{\sigma C_y}+1\right)} \tag{21}$$

$$a' = \frac{1}{\left(\frac{4F_P\sin(\varphi)\cos(\varphi)}{\sigma C_x}-1\right)} \tag{22}$$

equation is accurate in solving if the value of axial induction factor is less than 0.2 because above this value break down of simple momentum theory starts. Below scheme shows how different theories are valid for a range of axial induction factor values.

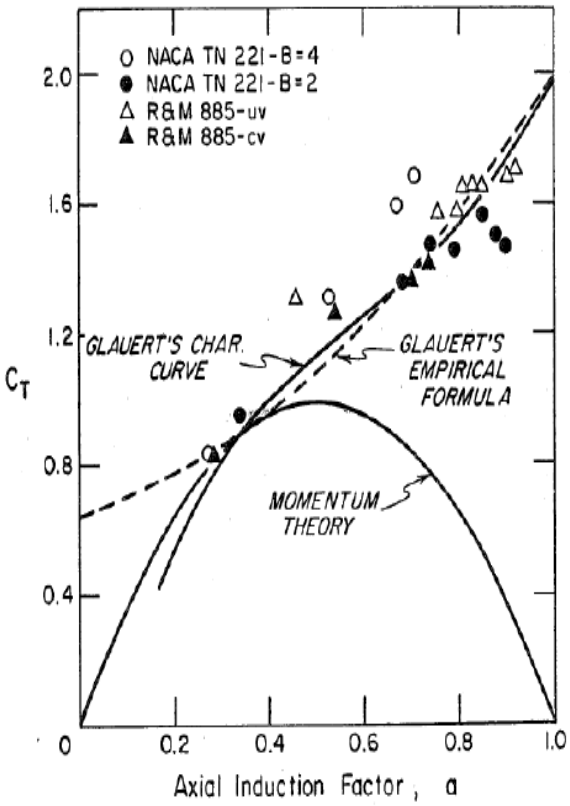

Fig. 6. Windmill Brake State Performance [5]

If the value of axial induction factor is found greater than 0.2, Glauert formulated a correction factor which is reformulated in terms of axial interference factor average [17]

$$a = \frac{1}{2}(2+K(1-2a_c \quad -\sqrt{(K(1-2a_c)+\Delta)+\tau(Ka_c^2)} \tag{23}$$

$$K = \frac{4F\sin^2(\varphi)}{\sigma C_y} \tag{24}$$

The following schemes takes the theory studied thus far is used in calculation of one ring element axial force and power in the rotor. The below figure shows a flow diagram tell us, how we did iteration to converge the axial and tangential induction factor for a single ring element. (relative wind speed angle) will be calculated in the next step and below equation is to be applied

$$\varphi = \tan^{-1}\left(\frac{(1-a)v_1}{(1+a')r\omega}\right) \tag{25}$$

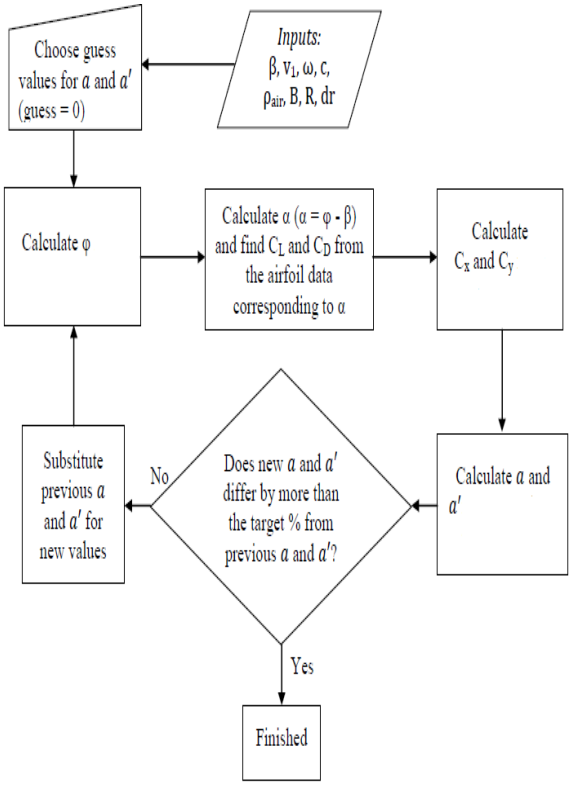

Fig. 7. Flow Diagram of the Iteration Process Used to Solve for Axial Induction Factor & the Tangential Induction Factor

After we find out the axial and tangential interference factor at converge solution, the torque and thrust for every blade segment is calculated by applying the below written equations:

$$T^*(r) = \frac{1}{2}\rho w^2 c C_x r \tag{26}$$

$$T_h^*(r) = \frac{1}{2}\rho w^2 c C_y \tag{27}$$

The overall axial force & power are calculated by applying the below equations:

$$T_h = B\int_0^R T_h^*(r)dr \tag{28}$$

$$P = \omega B\int_0^R T^*(r)dr \tag{29}$$

H. CFD

In this section, turbine blade Aerodynamics Analysis will be conducted in three-dimensional simulation using ANSYS Fluent. The three-dimensional simulation of blade geometry result will be compared with theoretical result which we get earlier from Blade element theory for validation of ours work.

Power	P	W	61.39
Efficiency	eta_r	%	87.21545
Torque	M	Nm	0.00145
Axial force	T	N	19.64560
Tip speed ratio	X_act	-	6.00000
Mean angle of attack	alpha_m	deg	4.37809

Fig. 8. Three-dimensional wind turbine modeling

Above shows our chosen parameters of wind turbine, our wind turbine is consisting of three blades and tip speed (optimal) ratio is 6, the rotational speed is 401.84 rpm when wind speed has reached to 5 m/s, under this condition, the power output of generator is 62 w.

I. Meshing

After working in geometry modular, moved towards meshing, we look up over geometry complexations. The flow passage of air through a rotating and twisted HAWT blade is much more complicated due to the angles of attack varying along the aero foil span. Meshing difficulty can be reduced by using unstructured grid which is usually use to mesh the turbine as it has very good adaptability. While we use structured grid was used to mesh the remaining of the computational domain as it has a nice meshing quality. Figure below shows that unstructured grids are found in rotational domain and structure grids are used in non rotating domain. Moreover, to improve the accuracy of simulation, the mesh size should be fine and intensive around the wind turbine blade surfaces. Because we all know that finer the size of the mesh more accurate will be the result. By keeping in mind, the following fact, we reduce the growth rate from 1.20 to 1.10 and change the element size to finer.

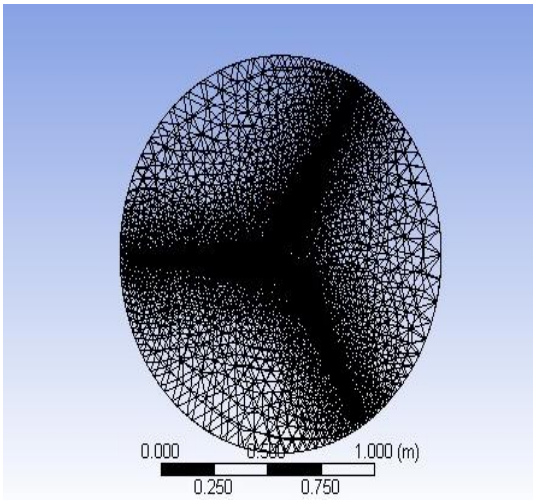

Fig. 9. Meshing of wind turbine blade

Fig. 9 shows that the mesh size is denser near the wind turbine blades and gets coarser when the mesh moves towards the boundaries. This meshing approach can capture the boundary layer near the wind turbine.

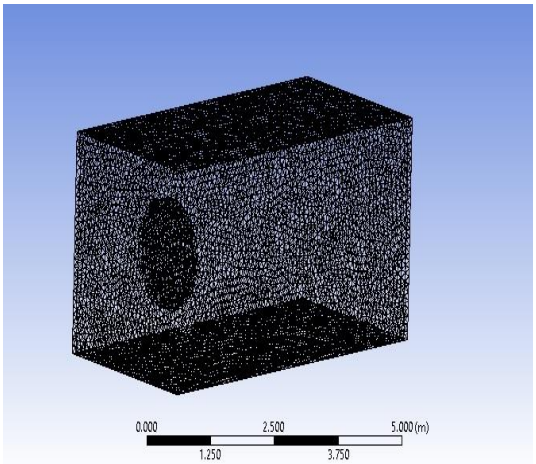

Fig. 10. Meshing of wind turbine

We use Pressure-based solver in Ansys Fluent and steady state solution of transient rotation were used for modelling of wind turbine. SST k- model was used, it includes many features which make result more accurate and precise for a wider class flows (adverse pressure gradient flows and aero foil). When simulation is over, coefficient of torque and thrust can be displayed and torque will be calculated by using value of coefficient of torque. Form this we can easily calculate the power using torque and angular speed relations.

IV. RESULTS

The Computational Fluid Dynamics and Blade Element Momentum theory results will be compared in this section. First coefficient of moment and coefficient of power are considered. From these results it is possible to conclude the short comings of the computational scheme. We can also investigate the deviation between them by examining the pressure distribution over the sections of blade and finding the integral tangential and axial forces. You can see the pressure distribution and velocity distribution diagram given below.

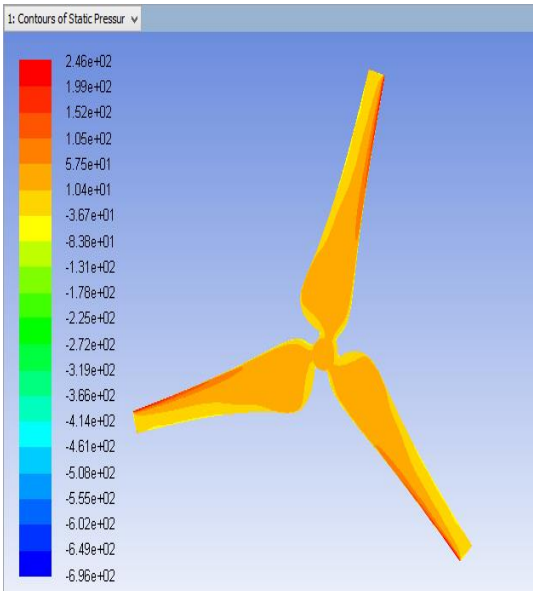

Fig. 11. Static Pressure contours

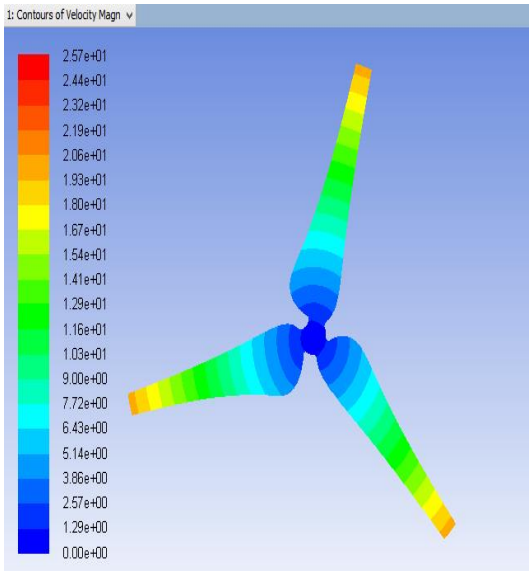

Fig. 12. Velocity contours

We obtain the results using the fine mesh simulations. Figure below compares the total output power for computations on the fine mesh and blade element theory mesh for 5 m/s inflow wind velocities. The differences in power range from 812%. We can do the mesh refinement but was not possible due to constraint on our computational

platform.

A. Comparison OF CFD with BEM

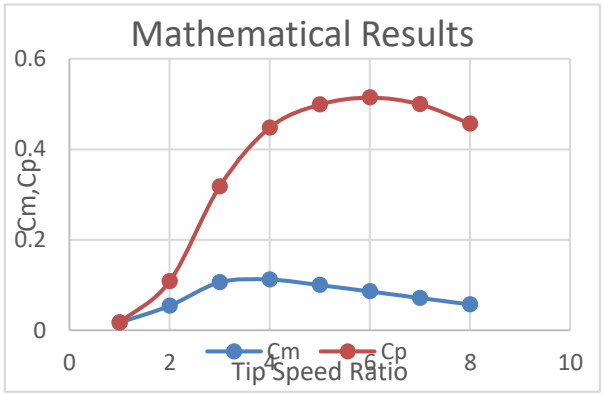

Fig. 13. Coefficient of power curves obtained by BEM

Below graph shows the comparison of coefficient of power curves that we obtained from the BEM and CFD. Two sets of curves are plotted in figure. The red curve represents the simulations based on input from the BEM turbine model. The black curve shows the CFD result in which the inlet wind speed was maintained at 5 m/s. From the power curve it is seen that the CFD and BEM models compare in relatively well manner.

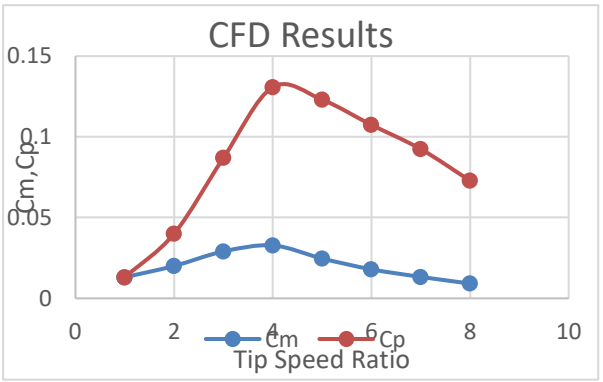

Fig. 14. Coefficient of power curves obtained by CFD

The result can be ascribed to the fact that deviation in our result is largely due to mesh size. We do not have a platform for doing meshing in our project

V. CONCLUSION

The wind turbine performance was looked overusing CFD and BEM. We first design the wind turbine chord distribution, operating RPM, twist, thickness using Blade Element theory and compared to CFD solutions at select certain points. Power curve generated from the CFD to the BEM was compared and we conclude that the BEM can be used in the variable rotational speed zone of wind turbine. We know that more power is generated by the outer sections of wind turbine as compared to hub. The results in variable pitch zone shows very much deviation between the CFD and BEM. The result can be ascribed to the fact that finer will be the mesh more accurate will be the result. We must do meshing in ICEM by manually doing the meshing use prism and tetra meshing on the surface to get the required result.

VI. LIMITATIONS AND FUTURE SCOPE

Although small scale wind turbines installation is not a cost-effective process, it does have a drawback. After a careful examination of the previous decade's efforts, we have arrived at this conclusion. We will now focus on some proposals that can be implemented in SSWTs future work with improved results. These are only hypothetical propositions; whether they will function in the actual world and give better results is dependent on the success of future trials. Fabricate the unit to corelate the analysis data. More input/output parameters, as well as metallographic analysis, should be included in future work.

REFERENCES

[1] M. Gul, N. Zulkifli, M. Kalam, H. Masjuki, M. Mujtaba, S. Yousuf, M. N. Bashir, W. Ahmed, M. Yusoff, S. Noor *et al.*, "Rsm and artificial neural networking based production optimization of sustainable cotton bio-lubricant and evaluation of its lubricity & tribological properties," *Energy Reports*, vol. 7, pp. 830–839, 2021. doi: https://doi.org/10.1016/j.egyr.2021.01.033

[2] M. Gul, M. Kalam, M. Mujtaba, S. Alam, M. N. Bashir, I. Javed, U. Aziz, M. R. Farid, M. T. Hassan, and S. Iqbal, "Multi-objective-optimization of process parameters of industrial-gas-turbine fueled with natural gas by using grey-taguchi and ann methods for better performance," *Energy Reports*, vol. 6, pp. 2394–2402, 2020. doi: https://doi.org/10.1016/j.egyr.2020.08.002

[3] M. Bashir, "A novel approach for integrating concentrated solar energy with biomass thermochemical conversion processes," Phd thesies, Aston University, 2017.

[4] H. T. Kadhim, K. Hussein, J. W. Salman, and N. Q. Farag. (2017) Design and building a rotor blade small wind turbine suitable for iraq's weather. [Online]. Available: https://bit.ly/3upBjTn

[5] R. A. Kishore and S. Priya, "Design and experimental verification of a high efficiency small wind energy portable turbine (SWEPT)," *Journal of Wind Engineering and Industrial Aero-*

dynamics, vol. 118, pp. 12–19, 2013. doi: https://doi.org/10.1016/j.jweia.2013.04.009

[6] M. M. Quazi, M. Ishak, A. Arslan, M. Fazal, F. Yusof, B. Sazzad, M. N. Bashir, and M. Jamshaid, "Mechanical and tribological performance of a hybrid MMC coating deposited on Al-17Si piston alloy by laser composite surfacing technique," *RSC Advances*, vol. 8, no. 13, pp. 6858–6869, 2018. doi: https://doi.org/10.1039/C7RA08191J

[7] M. M. Duquette and K. D. Visser, "Numerical implications of solidity and blade number on rotor performance of horizontal-axis wind turbines," *Journal of Soarl Energy Engineering*, vol. 125, no. 4, pp. 425–432, 2003. doi: https://doi.org/10.1115/1.1629751

[8] O. Siram, N. Sahoo, and U. K. Saha, "Wind tunnel tests of a model small-scale horizontal-axis wind turbine developed from blade element momentum theory," *Journal of Energy Resources Technology*, vol. 144, no. 6, p. 064502, 2022. doi: https://doi.org/10.1115/1.4052774

[9] A. Suresh and S. Rajakumar, "Design of small horizontal axis wind turbine for low wind speed rural applications," *Materials Today: Proceedings*, vol. 23, pp. 16–22, 2020. doi: https://doi.org/10.1016/j.matpr.2019.06.008

[10] M. Khaled, M. M. Ibrahim, H. E. A. Hamed, and A. F. AbdelGwad, "Investigation of a small horizontal–axis wind turbine performance with and without winglet," *Energy*, vol. 187, p. 115921, 2019. doi: https://doi.org/10.1016/j.energy.2019.115921

[11] P. Arumugam, V. Ramalingam, and K. Bhaganagar, "A pathway towards sustainable development of small capacity horizontal axis wind turbines–identification of influencing design parameters & their role on performance analysis," *Sustainable Energy Technologies and Assessments*, vol. 44, p. 101019, 2021. doi: https://doi.org/10.1016/j.seta.2021.101019

[12] R. E. Wilson, P. B. Lissaman, and S. N. Walker, "Aerodynamic performance of wind turbines. final report," Oregon State Univ., Corvallis (USA). Dept. of Mechanical Engineering, Tech. Rep., 1976.

[13] N. Karthikeyan, K. K. Murugavel, S. A. Kumar, and S. Rajakumar, "Review of aerodynamic developments on small horizontal axis wind turbine blade," *Renewable and Sustainable Energy Reviews*, vol. 42, pp. 801–822, 2015. doi: https://doi.org/10.1016/j.rser.2014.10.086

[14] R. K. Gupta, V. Warudkar, R. Purohit, and S. S. Rajpurohit, "Modeling and aerodynamic analysis of small scale, mixed airfoil horizontal axis wind turbine blade," *Materials Today: Proceedings*, vol. 4, no. 4, pp. 5370–5384, 2017. doi: https://doi.org/10.1016/j.matpr.2017.05.049

[15] W. Yossri, S. B. Ayed, and A. Abdelkefi, "Airfoil type and blade size effects on the aerodynamic performance of small-scale wind turbines: Computational fluid dynamics investigation," *Energy*, vol. 229, p. 120739, 2021. doi: https://doi.org/10.1016/j.energy.2021.120739

[16] A. Tummala, R. K. Velamati, D. K. Sinha, V. Indraja, and V. H. Krishna, "A review on small scale wind turbines," *Renewable and Sustainable Energy Reviews*, vol. 56, pp. 1351–1371, 2016. doi: https://doi.org/10.1016/j.rser.2015.12.027

[17] L. M. Kamp and L. F. Vanheule, "Review of the small wind turbine sector in kenya: Status and bottlenecks for growth," *Renewable and Sustainable Energy Reviews*, vol. 49, pp. 470–480, 2015. doi: https://doi.org/10.1016/j.rser.2015.04.082

[18] D. Strasszer and G. Xydis, "Cfd-based wind assessment for suburban buildings. the case study of aarhus university, herning campus," *Frontiers in Energy Research*, vol. 8, p. 351, 2020. doi: https://doi.org/10.3389/fenrg.2020.539095

[19] M. Bastankhah and F. Porté-Agel, "Experimental and theoretical study of wind turbine wakes in yawed conditions," *Journal of Fluid Mechanics*, vol. 806, pp. 506–541, 2016. doi: https://doi.org/10.1017/jfm.2016.595